Proceedings
of the 4th International Modelica Conference,
Hamburg, March 7-8, 2005,
Gerhard Schmitz (editor)

S. Wischhusen, G. Schmitz
*TUHH, Germany*
**Exergy-analysis of a direct-evaporating cooling plant with heat reclaim**
pp. 339-350

Paper presented at the 4th International Modelica Conference, March 7-8, 2005,
Hamburg University of Technology, Hamburg-Harburg, Germany,
organized by The Modelica Association and the Department of Thermodynamics, Hamburg University of Technology

# Exergy-analysis of a direct-evaporating cooling plant with heat reclaim

Stefan Wischhusen[1] Gerhard Schmitz
Hamburg University of Technology
Department of Thermodynamics
Denickestr. 17, D-21073 Hamburg
[1]wischhusen@tuhh.de

## Abstract

In this paper the modelling of a direct-evaporating two-stage cooling plant with the refrigerant ammonia (R717) will be described. The plant model is used to determine the power consumption as well as the possible heat reclaim to the domestic hot water system of the plant. In a sensitivity study important control parameters of the plant are evaluated for electricity, water and natural gas consumption. One characteristic operating point is investigated in an exergy-analysis [1, 2] to find potential for energy savings.

*Keywords: Refrigeration, Exergy-analysis, Heat recovery, Ammonia, R717, Two-stage system*

## 1 Introduction

Probably the largest application for industrial refrigeration is cooling and freezing of food. Large plants are needed to provide refrigeration throughout all seasons of a year covering all production steps during the processing, storage and transportation. Most of the plants are built in a direct-evaporating architecture where the refrigerant is evaporated in each cold storage or consumer. In contrast to that, indirect evaporation with a secondary cooling agent is used for air conditioning systems in large buildings. The reason for this is a lower pressure loss for liquid media in extensive pipework.

Historically, ammonia (R717) is one of the best known refrigerants in industrial applications and it has suitable properties like a high evaporation heat at moderate densities and a range of feasible saturation pressures at common working temperatures (especially with regard to low temperature applications). An economical advantage is its low price in comparison to other refrigerants. Drawbacks are the flammability and toxicity. Experiences go back to the 19th century when David Boyle (1873) and later Carl von Linde (1876) developed the first compression chillers using ammonia. The chiller created by Linde was used in breweries for cooling beer.

Since industrial refrigeration plants are operated many hours per year the energy consumption is relatively high and therefore capital investment for increasing the efficiency returns faster than in plain air conditioning plants which are just seasonally used. A dynamic simulation is carried out because of the high refrigerant and water capacity of the plant.

## 2 Refrigeration Plant Topology and Functioning

In order to provide cooling capacity at two temperature levels (-10 °C and -35 °C) the compression of the working fluid is separated into two stages: The high pressure (13.5 bar/2.91 bar) and the low pressure (2.91 bar/0.9 bar) cycle, displayed in Fig. 1. The low pressure compression provided by two screw compressors (“Booster”, 1 → 2) can be operated independently while one high pressure compressor is always needed to reject the waste heat over the condensers. Therefore, a higher cooling capacity is always necessary on the high pressure side with three screw compressors installed (3 → 4). The waste heat is mainly rejected to the ambience by evaporative condensers, which incorporate air and water for evaporative cooling (5 → 6,7).

Since there is a high demand for domestic hot water (DHW) in the plant during production times (mass

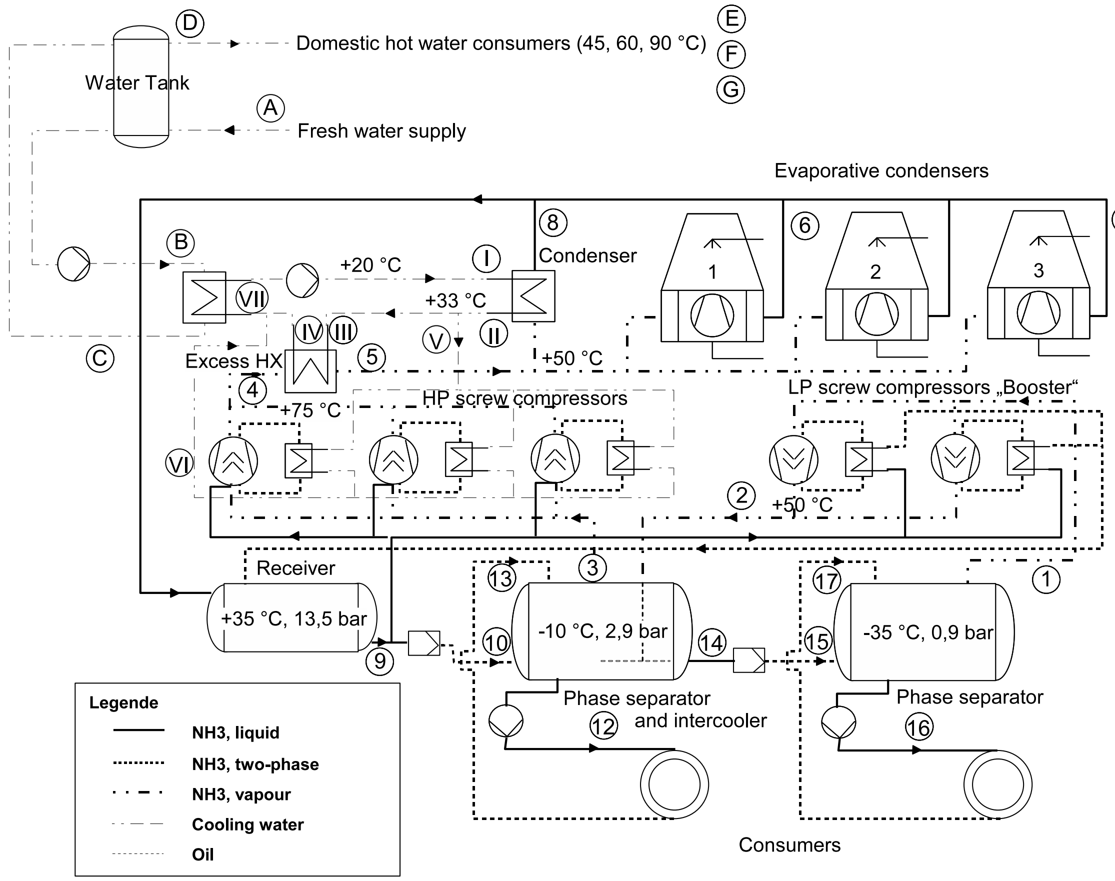


Figure 1: Simplified plant schematic including the refrigeration and domestic hot water system

flow rates are as high as 8 kg/s) it is convenient to recover waste heat by cooling compressor oil and high pressure gas in a water-cooled excess heat exchanger (4 → 5) and a water-cooled condenser (5 → 8). Those heat exchangers (HX) are of shell and tube type. Following German domestic water ordinance the heat exchangers have to be cooled indirectly to avoid a contamination with ammonia in case of leakage. Subsequently, the condensate flow is fed into the high pressure receiver (V=2 $m^3$, 8 → 9) where it can be tapped for expansion or cooling the low stage and high stage screws (9). The latter compressors (3 → 4) just draw liquid ammonia when the cooling water temperature is too high to ensure an oil temperature of 48 °C. Like oil the liquid ammonia may be injected into the suction side of the compressor to decrease the outlet temperature of the compressed gas. To remove the oil fraction from the superheated refrigerant vapour, an oil separator for each compressor is necessary which is also used as a tank storage.

Unlike in one-stage refrigeration systems, the expanded refrigerant is first stored in a phase separator (V=11 $m^3$, each) to remove flash gas. This component is essential in order to supply pure liquid medium to the pumps and evaporators of each stage. The separating vessel on the intermediate pressure level (10,13 → 3,12,14) is equipped with an intercooler because of the superheated low stage gas which needs to be cooled down to saturation conditions before it can be compressed again by the screws of the second stage.

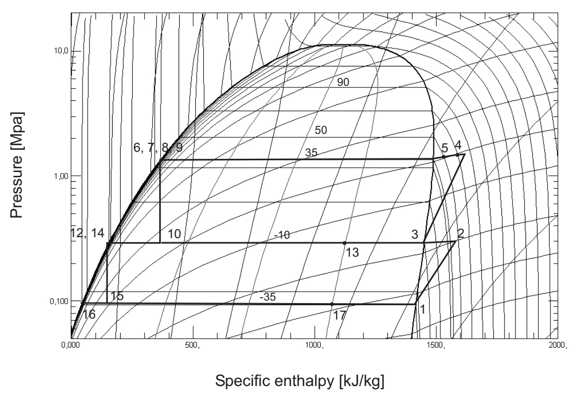


Figure 2: p,h-diagram for R717 of the two-stage refrigeration system – Arabic numerals with regard to Fig. 1

In applications with temperatures below 4 °C a defrost system has to be applied to each cooling coil which is in contact with (humid) air. For this purpose superheated refrigerant tapped before the excess HX is used occasionally by switching a valve at each evaporator.

The total cooling capacity of the screw compressors is 847 kW on the low stage (-35 °C) and 2308 kW on the high pressure side whereof 1461 kW are available for -10 °C consumers. The rated power consumption of the compressor motors sums up to 200 kW for the Boosters and 693 kW on the high stage. Accordingly, the evaporative and water-cooled condensers have a cooling capacity of 3910 kW (incl. desuperheat HX) at a saturation temperature of +35 °C.

The capacity control of the system is realised by a variable valve in the screw compressors which can throttle the effective mass flow rate at constant speed. The lowest continuous working point is limited to 10 % of the rated capacity. Below that operation point the motor is driven in an on-off procedure. Internally, the oil flow is adjusted so that a constant oil inlet temperature can be provided. The mass flow rate of oil is almost of the same magnitude as the refrigerant flow to ensure a sufficient lubrification, sealing and cooling. All compressors are organised in a load dependent cascade, operating as many machines as needed.

In an analogous manner the three evaporative condensers are enabled in an pressure dependent cascade at operating points ranging from 9 to 12 bar. At low pressures, the spray water pumps are activated followed by the ventilation of the cooling towers. The mass flow rate through the parallel condensers and cooling towers is adjusted naturally since a lower heat transfer rate leads to higher pressure losses due to the rising resistance in one branch.

The refrigeration process is also shown in a logarithmic p,h-diagram for $NH_3$ in Fig. 2.

## 3 Boundary Conditions and Measurements

Since the cooling demand is changing dynamically the plant is not driven continuously but in a typical load profile (see Fig. 4) which is dominated on the low pressure side (-35 °C) by shock-cooling of food entities (2250 hours/a) and on the medium pressure side by cooling storage rooms at -10 °C (8760 hours/a) (see Fig. 3). The load profile of the low temperature consumers varies between 30 and 1100 $kW_{th}$ and for the normal cooling between 100 and 2300 $kW_{th}$. Thanks to the data measurement of the plant's operator the hourly power and water consumption (see Fig. 4) as well as the product flow of the plant is known and it is considered as boundary conditions for the system simulation. Since the unknown cooling requirement is an important input variable of the load dependent simulation it has to be calculated from known and assumed variables like the power consumption and the product flow. On the low temperature side (LT, 16 → 17) the refrigeration load can be estimated by the following equation:

$$\dot{Q}_{0,\,LT} = \dot{n}_{prod} \cdot 11\ \mathrm{kJ} + \dot{Q}_{0,\,aux} \qquad (1)$$

where $\dot{n}_{prod}$ denotes the flow rate of product. Each product entity has a heat capacity of 11 kJ in the corresponding temperature range and $\dot{Q}_{0,\,aux}$ stands for the smaller amount of additional refrigeration which averages 30 kW. The refrigeration load for room cooling $\dot{Q}_{0,\,MT}$ (12 → 13) at an evaporation temperature of $\vartheta_0$ =-10 °C results from the following equation

$$\dot{Q}_{0,\,MT} = P_{el} \cdot \overline{COP} - \dot{Q}_{0,\,LT} \qquad (2)$$

applying an average coefficient of performance $\overline{COP}$ =3. Despite the fact that the peak load of both stages sums up to 3,400 kW (see Fig. 3) their occurrence is separated. The highest total load is not larger than 2,450 kW.

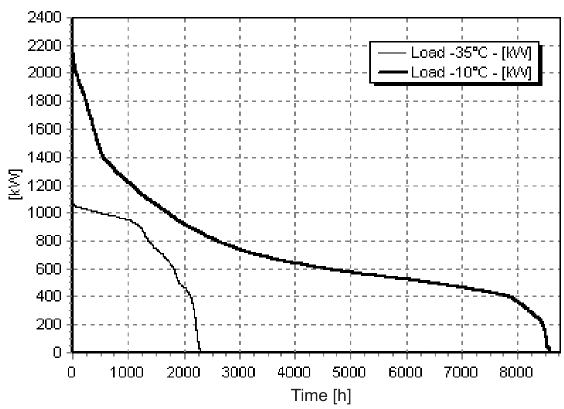


Figure 3: Annual load duration curve for refrigeration

Not available are ambient conditions for that time, so that weather data from a test reference year of the corresponding region in Germany has been used to

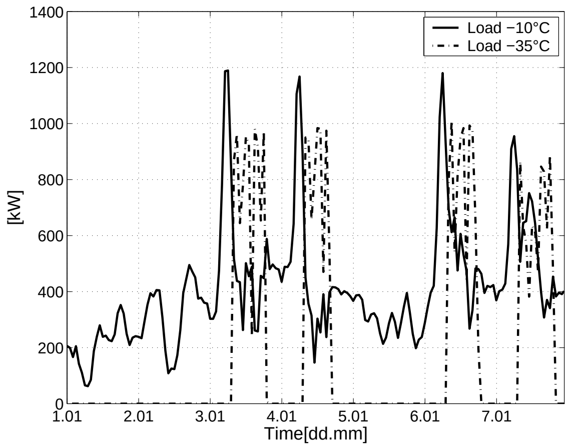


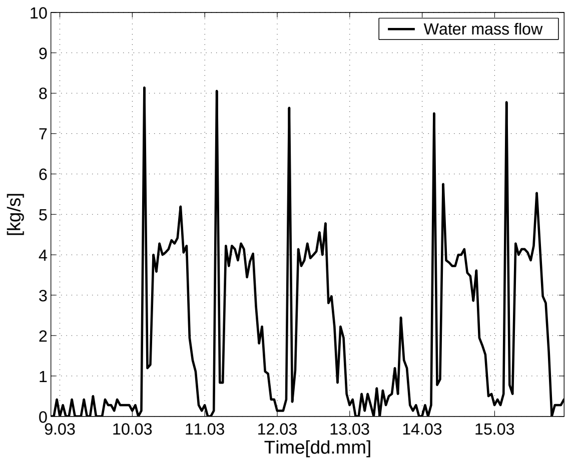


Figure 4: Typical cooling requirement (t.) and DHW consumption profile (b.)

calculate the performance of the cooling tower model (temperature and relative humidity as inputs). The temperature of the fresh water was assumed to change in a sinusoidal way between 10 °C at the beginning of spring and 13 °C in late summer.

The mass flow rate of consumed domestic hot water (E,F,G) is also dynamically changing. The highest flow rates occur at the beginning of each production day (see Fig. 4). Those days are contemporaneously characterised by a high cooling demand on the low temperature side because of the necessary product cooling. This fact combined with a considerable water demand during production times results in a very worthwhile potential for heat recovery. On the other hand the mass flow rate of water in the meantime is not high enough to provide a sufficient condensation and cooling capacity.

Important for an economical analysis of an existing plant are the energy and media prices which are listed below:

- Electricity cost: 70 €/MWh (Compressors, cooling towers, pumps),
- Gas price: 35 €/MWh (DHW supply),
- Fresh water cost: 0.89 €/m$^3$ (Cooling towers),
- Charge for waste water: 2.29 €/m$^3$ (Cooling towers).

## 4 Modelling of Plant and Components

First of all it should be pointed out, that the modelling in this case was focused on the simulation of the refrigeration plant with the integration of the heat recovery. The models for hydronic systems have been supplied by the model libraries of HKSim [3, 4, 5]. Pfafferott has shown that a dynamic simulation of mobile refrigeration systems is possible [6]. He used Modelica for modelling of thermohydraulic elements integrating dynamic energy and mass balances and a quasistatic impulse balance. Unfortunately, such detailed component models are not suitable for complex systems, especially when long simulation periods are investigated. The typical period in the current project is one week and more in order to detect improvements and present them in a financial suitable resolution.

When applying the Finite Volume method in fluid modelling it is important to have a medium property model for all technical relevant states. This is given by a fundamental equation of state which was elaborated by Baehr and Tillner-Roth for a few important refrigerants [7] also including R717. The two-phase region has to be modelled by polynomial functions which depend on one thermodynamic state variable ($T$ or $p$). It is known that the simulation of the gaseous and two-phase region can be rather efficiently performed, when the density $\rho$ (or the specific volume $v$, resp.) and the temperature $T$ are used as states and inputs to the highly non-linear equations. The dimensionless Helmholtz-function is defined as:

$$\Phi := f(T,v) \cdot \frac{1}{RT}. \tag{3}$$

Provisions have to be made with regard to the calculation of liquid state properties. In this region the simulation may become stiff since small changes (or even integration failures) in temperature at nearly

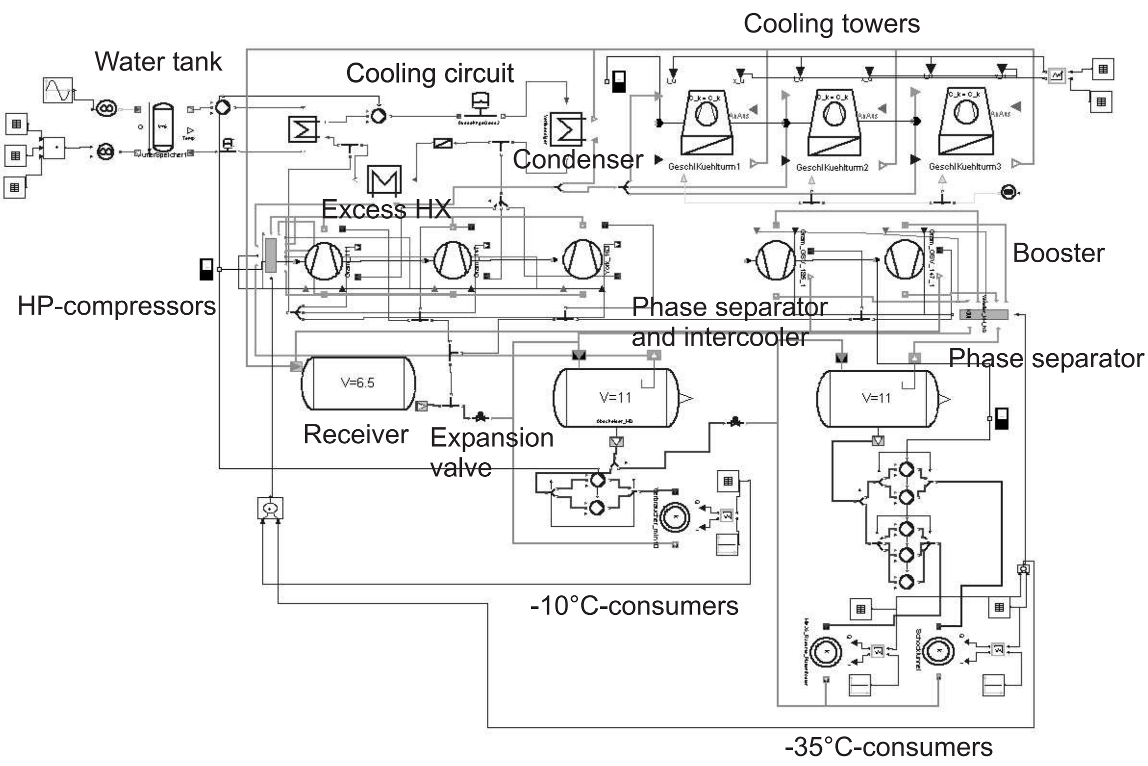


Figure 5: Plant model integrating the two stage refrigeration cycles, cooling water circuit and fresh water tank

constant density result in large pressure gradients. Those gradients lead to small system time constants due to the linkage of momentum and mass and energy balance. This is one reason why a state variable selection of pressure $p$ and specific enthalpy $h$ is generally preferred. However, with those states an iterative calculation of $T$ and $v$ is necessary during the simulation because the complex property functions can not be transformed symbolically, yet. In order to optimise the simulation also with respect to simulation speed it was decided to use a component related formulation of the balance equations in this project especially regarding components containing liquid refrigerant (e. g., refrigerant pumps and other hydraulic elements). One important and simplifying assumption is, that industrial plants are operated more or less continuously even though with variable utilisation factor. Therefore, heat and mass dissipation is not taken into account. From this fact follows that the feed ducts of the evaporators are always passed through with liquid medium. For those elements the incompressible formulation of the mass and energy balance [4] may be used with a constant specific heat capacity $c$ =4,500 J/(kg·K) and a constant density of $\rho$ =650 kg/m$^3$.

Very important for achieving a fast and stable simulation is also a component related momentum balance which should be as simple as possible. A momentum balance is always needed when a mass shift inside the system due to pressure gradients has to be calculated. In other words: It can be expressed ideally and more efficient if the mass transfer is guarded by a superior control system. For example, the mass flow through the expansion valve of each stage is set in order to realise a constant liquid fill level in the following phase separator.

The mass flow rates through the parallel passes of the condenser and cooling towers just depend on the pressure loss across each branch (in steady state always the same value) which is defined by hydraulic pressure drop correlations. For the quasistatic momentum balance follows:

$$0 = p_{in} - p_{out} - \Delta p_{loss} \tag{4}$$

$$\Delta p_{loss} = \Delta p_{100} \cdot \left(\frac{\dot{m}}{\dot{m}_{100}}\right)^2 \cdot \frac{\rho_{100}}{\rho} . \tag{5}$$

All parameters indicated by 100 in Eq. 5 refer to one characteristic operation point. The density factor can not be neglected when the liquid fraction is variable or a dry out of the heat exchanger is possible (here: condenser). This is often the case in the actual plant when the cooling water temperature rises due to a low domestic hot water consumption.

Moreover, component models which show a phase change like condensers and evaporators should not be separated into multiple volumes to avoid too many events during simulation. A promising approach could be a Moving-Boundary-Model [8] although it was not implemented in this work because of the frequent dry out of the condenser and the load dependent evaporator model ($\dot{Q}_0$ is an input variable).

The heat transfer rate from the refrigerant to the liquid water in the water-cooled condenser is calculated by a quasistatic efficiency calculation ($P_1$-NTU) from [9].

$$\dot{Q}_{liq} = P_1 \cdot C_{min} \cdot \left(T_{in}^{liq} - T_{out}^{liq}\right) \quad , \quad C = c \cdot \dot{m} \qquad (6)$$

$$P_1 = \begin{cases} \dfrac{2}{1+\frac{C_{min}}{C_{max}}+\sqrt{1+\frac{C_{min}}{C_{max}}^2}\cdot\coth\left(\sqrt{1+\frac{C_{min}}{C_{max}}^2}\cdot\frac{NTU}{2}\right)} \quad , \\ \quad \mathrm{C}_{max} > 0 \;\;\&\;\; \frac{C_{min}}{C_{max}} < 1 \;\;\&\;\; \mathrm{C}_{min} > 0\,. \\ \dfrac{1}{1+\coth\left(\frac{NTU}{\sqrt{2}}\right)} \quad , \\ \quad \mathrm{C}_{max} > 0 \;\;\&\;\; \frac{C_{min}}{C_{max}} >= 1 \;\;\&\;\; \mathrm{C}_{min} > 0\,. \end{cases} \qquad (7)$$

Since the specific heat capacity at constant pressure $c_p$ is equal to infinity in the two-phase region, a crossing function has to be implemented realising a "chatter-free" solution when liquid or vapour content is high. Good experiences were made with a tanh-function changing its value and derivation steadily at vapour qualities $x = 0\ldots\ 0.05$ and $x = 0.95\ldots\ 1$. The value of the function is multiplied with the property value for the specific heat capacity of the property model.

The compressors are modelled in a Super-Model approach integrating the base compressor model, an oil separator, the water-cooled oil heat exchanger (fixed properties for liquid oil) and the auxiliary liquid ammonia injection (see Fig. 6). Instead, the booster model incorporates an oil cooling heat exchanger permanently fed with ammonia.

A determining factor for the power consumption of the plant is the efficiency of the compressor. The so called coefficient of performance (COP) mainly depends on

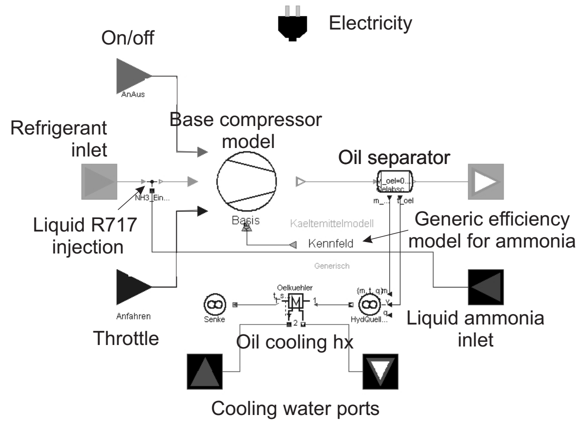


Figure 6: Diagram layer of a high pressure screw compressor model with integrated oil separator, oil cooler and ammonia injection

the part load control (part load factor $\varphi$) and the thermodynamic properties of the refrigerant as well as the thermodynamic states in the suction and discharge chamber. The latter mainly result from the actual heat transfer of all components in the cycle. With regard to this plant the suction (index *suc*) and discharge (index *dis*) pressure is defined by the capacitive component models (e. g., the excess heat exchanger and the phase separator in the high pressure cycle, see Fig. 5). In order to calculate the power consumption the mentioned thermodynamic variables are considered in the calculation of the total efficiency of the compressor.

$$\begin{aligned} COP \quad = \quad & f_{pl}\left(\Delta p, \varphi\left(p_{suc}, p_{dis}, \frac{\dot{m}}{\dot{m}_{max}}\right)\right) \\ & \cdot f_{th}\left(p_{suc}, p_{dis}, \dot{Q}_0^{nom}, P_{el}^{nom}, \eta_{mech}\right) \quad (8) \end{aligned}$$

The part load function $f_{pl}$ may be derived from manufacturer data or from literature [10]. For the calculation of the rated performance (index *rat*) at variable suction and discharge pressures ($f_{th}$) a determination of the refrigerant's properties (specific enthalpies $h$, entropies $s$ and densities $\rho$) is carried out. In contrast to the *rated* performance at **full** mass flow rate and **variable** pressures the *nominal* performance denotes **one** rated operating point at **constant** pressures.

$$f_{th} = \frac{h_{0,\,in} - h_{0,\,out}}{h_{dis}^{is} - h_{suc}} \cdot \eta_{is} \cdot \eta_{mech} \qquad (9)$$

$$\eta_{is} = \frac{\dot{m}^{rat} \cdot \left(h_{dis}^{is} - h_{suc}\right)^{rat}}{P_{el}^{nom}\eta_{mech}} \qquad (10)$$

$$\dot{m}^{rat} = \frac{\rho_{suc}}{\rho_{suc}^{rat}} \cdot \dot{m}^{nom} \qquad (11)$$

$$\dot{m}^{nom} = \frac{\dot{Q}_0^{nom}}{h_{0,\,in} - h_{0,\,out}} \tag{12}$$

$$h_{dis}^{is} = h\left(s\left(h_{suc}, p_{suc}\right), p_{dis}\right) \tag{13}$$

It is assumed that the isentropic efficiency of the compression at nominal mass flow rate $\dot{m}^{nom}$ is nearly constant for all operating points. In addition, the available enthalpy of evaporation is assumed to be ideally used.

$$h_{0,\,in} = h_{liq}(p_c) \tag{14}$$

$$h_{0,\,out} = h_{vap}(p_0) \tag{15}$$

At very low cooling requirements (10 % of $\dot{Q}_0^{rat}$) the control system of the compressors stops the continous operation and activates a two-point control with a minimum mass flow rate.

For achieving an efficient simulation only the largest capacities in the cycle were modelled by control volumes. Those components are the phase separators (each 11 m$^3$) and the high pressure receiver (2.3 m$^3$). Additionally, the high pressure heat exchangers were also modelled by using dynamic mass and energy balances in order to stabilise the solution of the non-linear system of equations during simulation. The modelling of the intercooler functionality of the phase separator on the intermediate pressure level is realised by mixing of all inbound enthalpy flows and computing saturated enthalpies for all outgoing mass flows.

A very demanding component from the modelling point of view is the evaporative condenser which has three fluid fluxes moving in different directions (Refrigerant: horizontal, air: bottom-top, water: top-bottom). A detailed model is described by [11, 12]. More applied to the needs of complex energy system simulations seems to be the approach of Stabat and Marchio [13] which offers a promising approach and some successful validation.

The model of this study is even more simplified by using the assumption that the air outlet condition equals always the mean temperature between the entering refrigerant and the wet bulb temperature while the relative humidity is constant. The cooling capacity can be adjusted by a variable mass flow rate of air. The supplied characteristic curve for the ventilation yields the power consumption of the motor.

## 4.1 Validation of the Plant Model

For the validation of the plant model measurement data has been supplied by the plant operator. The data displays the power, domestic water consumption and waste water flow in an hourly interval. Moreover, some offline-information was collected on a visit of the plant while the production was on (high cooling requirement for -35 °C-consumers).

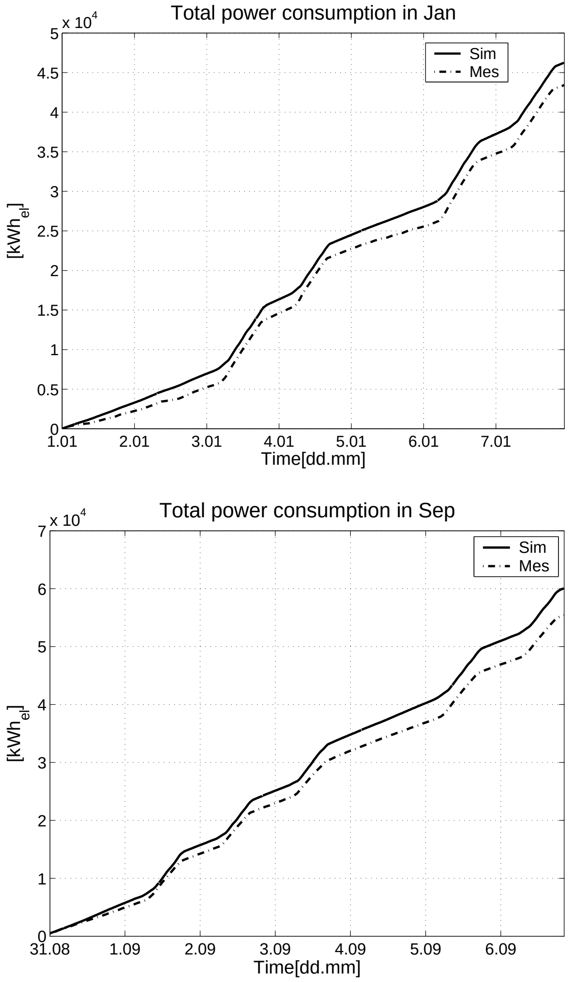


Figure 7: Comparison of the total power consumption in January (t.) and September (b.) with simulation results

The comparison of the power consumption shows a good agreement. In both simulated periods of one week in January and September respectively the simulation result is slightly higher than the measurement. The relative deviation is less than 7.7 % (Fig. 7). Obviously, the power consumption of the plant is overpredicted when the production cooling is off .

| Item | Measurement 29.04.04, 13:00 | Simulation 23.05.03, 13:00 |
|---|---|---|
| **Heat reclaim** | $\vartheta$ [°C] | $\vartheta$ [°C] |
| HX "Excess", water | 25 / 38 | 29 / 37 |
| HX "Condenser", water | 20 / 28 | 17 / 29 |
| HP screw 1, oil | 52 | 45 |
| HP screw 1, gas | 70 | 60 |
| HP screw 3, oil | 55 | 45 |
| HP screw 3, gas | 68 | 63 |
| **Receiver** | $p_c$ [bar] | $p_c$ [bar] |
| Conden. pressure | 11.5 | 11.7 |
| **Aux.** | | |
| Ambient temp. | 20 °C | 20 °C |

Table 1: Comparison of temperatures and pressures for one operating point with comparable boundary and load conditions

In Tab. 1 some temperatures and pressures displayed by onboard information systems or thermometers are listed for one operating point in April. Those values were compared to the corresponding values of the plant simulation at a similar load condition of the previous year. Especially, the simulated saturation pressure in the condensers, responsible for the attainable heat recovery, matches the value of the measurement. The same applies for the cooling water temperatures in the excess and condensing heat exchanger. A greater deviation can be seen in the gas and oil temperatures of the high pressure compressors. It must be pointed out that the position of the oil temperature sensor could not be clarified. Hence, the model of the oil cooling unit was not calibrated again but the parameters of the plant documentation were used.

## 5 Exergy-analysis of the Refrigeration System

For estimating savings potential it is important to know where the dominating loss mechanisms of a process are located. Such losses may be noticed in form of heat transfer, power decrease, mixing and pressure resistances. For the purpose of a clear description of process efficiencies it is necessary to define how much of an energy portion can be transformed into any other form of energy. For example, it is not possible to transfer heat from a cooler to a warmer volume in order to produce power. It is even not permitted by the second law of thermodynamics to completely turn heat into power by reducing the temperature of a medium to ambient conditions. The exergy $E$ represents that part of energy which is technically useful and can be extracted without restrictions to work. The specific exergy $e$ is expressed by:

$$e = \underbrace{h - h_0 - T_0\,(s - s_0)}_{\text{thermal}} + \underbrace{0.5(c^2 - c_0^2)}_{\text{kinetic}} + \underbrace{g(H - H_0)}_{\text{potential}} \qquad (16)$$

The (specific) exergy always depends on the definition of ambient conditions indicated by the index 0. It is not always trivial to select the "correct" ambience model and the discussion about this issue is not finished, yet. Nevertheless, the exergy represents a powerful tool for analysing energy systems.

| Item | Total change of exergy flow $\Delta\dot{E}^{tot}$ [kW] | Inner cost flow $\dot{K}^i$ [€/h] |
|---|---|---|
| 1 → 2 | -62.15 | -4.60 |
| 3 → 4 | -142.42 | -10.58 |
| 4 → 5 | -12.10 | -0.90 |
| 5 → 6 | -92.02 | -6.83 |
| 5 → 7 | -44.30 | -3.29 |
| 5 → 8 | -8.48 | -0.63 |
| 6,7,8 → 9 | 2.50 | 0.19 |
| 9 → 10 | -23.98 | -1.78 |
| 10,2,13 → 3,14 | -11.96 | -0.89 |
| 12 → 13 | -47.18 | -3.50 |
| 14 → 15 | -4.24 | -0.31 |
| 15,17 → 1,16 | -0.76 | -0.06 |
| 16 → 17 | -195.33 | -14.50 |
| Total | -642,42 | -47.68 |

Table 2: Inner costs resulting from exergy losses without heat reclaim for one hour continuous operation (see Fig. 1 for items) – The specific cost for exergy is 0.074 €/kWh$_{ex}$

In order to express the exergy losses in the corresponding components in terms of hourly costs the change of exergy is calculated first for an characteristic operating point with active production cooling. The cooling requirement is 485 kW for storage rooms (-10 °C) and 985 kW for production (-35 °C). At the same time a domestic hot water consumption of 4.5 kg/s takes place. Kinetic and potential forms of exergy are neglected and the reference point is set to $p_0$ = 1 bar

| Item | Thermal change of exergy flow $\Delta\dot{E}^i$ [kW] | Power consump. $P_{el}$ [kW] | Change of enthalpy flow $\Delta\dot{H}$ [kW] | Water consump. $\dot{m}_{fr}$ [kg/s] | Waste water flow $\dot{m}_A$ [kg/s] | Outer cost flow $\dot{K}^o$ [€/h] |
|---|---|---|---|---|---|---|
| 1 → 2 | 104.15 | 166.30 | 145.63 | 0.00 | 0.00 | 11.64 |
| 3 → 4 | 255.18 | 397.60 | 173.09 | 0.00 | 0.00 | 27.83 |
| 4 → 5 | -12.10 | 0.00 | -80.64 | 0.00 | 0.00 | 0.00 |
| 5 → 6 | -53.02 | 39.00 | -1056.08 | 0.31 | 0.08 | 4.58 |
| 5 → 7 | -25.10 | 19.20 | -494.50 | 0.15 | 0.04 | 2.21 |
| 5 → 8 | -8.48 | 0.00 | -166.95 | 0.00 | 0.00 | 0.00 |
| 6,7,8 → 9 | 2.50 | 0.00 | 0.00 | 0.00 | 0.00 | 0.00 |
| 9 → 10 | -23.98 | 0.00 | 0.00 | 0.00 | 0.00 | 0.00 |
| 10,2,13 → 3,14 | -11.96 | 0.00 | 0.00 | 0.00 | 0.00 | 0.00 |
| 12 → 13 | -41.18 | 6.00 | 485.76 | 0.00 | 0.00 | 0.42 |
| 14 → 15 | -4.056 | 0.00 | 0.00 | 0.00 | 0.00 | 0.00 |
| 15,17 → 1,16 | -0.76 | 0.00 | 0.00 | 0.00 | 0.00 | 0.00 |
| 16 → 17 | -181.03 | 14.30 | 983.26 | 0.00 | 0.00 | 1.00 |
| VII → I | -19.03 | 0.70 | -372.68 | 0.00 | 0.00 | 0.05 |
| I → II | 5.46 | 0.00 | 169.24 | 0.00 | 0.00 | 0.00 |
| III → IV | 5.15 | 0.00 | 87.59 | 0.00 | 0.00 | 0.00 |
| V → VI | 10.52 | 0.00 | 115.04 | 0.00 | 0.00 | 0.00 |
| IV,VI → VII | -2.08 | 0.00 | 0.00 | 0.00 | 0.00 | 0.00 |
| B → C | 13.42 | 0.70 | 370.97 | 0.00 | 0.00 | 0.05 |
| C → D | -0.68 | 0.00 | 0.00 | 0.00 | 0.00 | 0.00 |
| D → E | -8.97 | 0.00 | 106.32 | 0.00 | 0.00 | 40.93 |
| D → F | -25.42 | 0.00 | 241.12 | 0.00 | 0.00 | 92.83 |
| D → G | -12.85 | 0.00 | 89.23 | 0.00 | 0.00 | 34.35 |

Table 3: Change of exergy and enthalpy flow rate for the refrigerant, power and water consumption, waste water mass flow rate and outer cost flow invested - power rates and media prices are listed in Sec. 3

and $\vartheta_0$=12.4 °C (fresh water temperature entering the plant). The change of exergy and enthalpy with regard to the refrigerant or cooling water flow is shown in Tab. 3. An increase of exergy ($\Delta\dot{E}^i > 0$) happens in the compressors and in those heat exchanger volumes which show a rising temperature (cooling water HX). Under the assumption of continuous operation for one hour the plant consumes a total of 643.8 kWh exergy in form of electricity. This effort has to be compared to the thermal profit of the plant which is defined by the exergy provided by the evaporators and the water tank to the DHW system. Hence, the exergetic efficiency $\zeta$ follows from the ratio of the actual thermal advantage to the total exergy input ($\sum P_{el}$):

$$\zeta = \frac{\sum \dot{E}_Q}{\sum P_{el}} = \frac{|\Delta\dot{E}^i_{12,13}| + |\Delta\dot{E}^i_{16,17}| + \Delta\dot{E}^i_{B,D}}{\sum P_{el}} = 0.36 \tag{17}$$

This value is more plausible than the COP which equals 2.28 at the same time. If an economical analysis shall be carried out it is possible to combine the change of exergy flow rate $\Delta\dot{E}^i$ with outer cost flows $\dot{K}^o$ (see Tab. 3) resulting from power and water consumption. This method is described as “exergy costing” by Bejan [1]. In a simplifying approach it can be postulated that all outer costs are divided by the exergy input in order to calculate the specific costs of exergy. With this average value the costs of internal losses are expressed (see Tab. 2). Generally, the initial costs (e. g. capital investment) should also be included but in this case an operating plant is considered and it should be investigated how the efficiency could be improved without installing new components. Therefore, the task was not to compare different components with different initial costs and thus this contribution was neglected.

The total amount of all costs for this operation mode is 48 €/h. The largest cost centre in terms of exergy destruction is encountered in the cooling towers (10 €/h) followed by the expansion valves (2.10 €/h) and the phase separator of the high stage (0.89 €/h) due to the internal heat transfer. Hence, financial savings can be obtained by reducing exergy destruction in the evaporative condensers (e. g. by lowering the saturation pressure or increasing the mass flow rate through the water-cooled condenser).

| Item | Cost flow $\dot{K}^i$ [€/h] | Revenue $\dot{G}$ [€/h] | Virt. op. profit $\dot{P}$ [€/h] |
|---|---|---|---|
| $1 \rightarrow 2$ | -4.60 | 0.00 | -4.60 |
| $3 \rightarrow 4$ | -10.58 | 4.39 | -6.19 |
| $4 \rightarrow 5$ | -0.90 | 3.34 | 2.44 |
| $5 \rightarrow 6$ | -6.83 | 0.00 | -6.83 |
| $5 \rightarrow 7$ | -3.29 | 0.00 | -3.29 |
| $5 \rightarrow 8$ | -0.63 | 6.46 | 5.83 |
| $6,7,8 \rightarrow 9$ | 0.19 | 0.00 | 0.19 |
| $9 \rightarrow 10$ | -1.78 | 0.00 | -1.78 |
| $10,2,13 \rightarrow 3,14$ | -0.89 | 0.00 | -0.89 |
| $12 \rightarrow 13$ | -3.50 | 0.00 | -3.50 |
| $14 \rightarrow 15$ | -0.31 | 0.00 | -0.31 |
| $15,17 \rightarrow 1,16$ | -0.06 | 0.00 | -0.06 |
| $16 \rightarrow 17$ | -14.50 | 0.00 | -14.50 |
| Total | -47.68 | 14.20 | -33.48 |

Table 4: Costs due to exergy losses and destruction, revenue of heat recovery and virtual operating profit in comparison to conventional system for one hour continuous operation – The specific gain of recovered heat is 0.039 €/kWh$_{th}$

Useful changes of exergy in the evaporators cost 18 €/h so that this can be considered as the minimum running cost level if the insulation of the rooms or other consumers could not be further improved.

Up to now the positive impact of the heat reclaim is missing in this study. To attain the total balance of costs and revenues the gas savings from the DHW system are propagated *upstream*. By means of cooling water a total of 371 kW waste heat is recovered from the ammonia or oil, respectively. This is almost 20 % of the waste heat produced by the cycle. 115 kW are contributed by the oil coolers (6 %) and 80 kW (4 %) by the excess heat exchangers. Helmke [14] even states a potential of 7.4 % for excess heat and 9.2 % for oil cooling (only high pressure screws).

The actual heat recovery depends strongly on the availability of cooling water which has only low temperatures in case of DHW consumption. In order to supply the demand of hot water (45 °C, 60 °C and 90 °C) a heating capacity of 807 kW is needed. Assuming an efficiency of 90 % for heating and specific heat costs of 0.039 €/kWh$_{th}$ the running costs of a conventional plant would be 31.07 €/h. Taking the recovered heat into account the costs for natural gas drop to under 17 €/h and therefore the heat exchangers for heat reclaim are not representing a loss of 1.50 €/h but a *virtual operating profit* of 8.20 €/h. In addition, the oil coolers also show a revenue of 4.39 €/h reducing the loss of the HP screws from 10.58 €/h to 6.19 €/h. A complete coverage of the DHW supply by the refrigeration system is not possible as long as temperatures of more than 60 °C are needed. But it would be possible to realise higher savings (see Tab. 4) if a consumer of 1.913 kW at a low temperature of approx. 30 °C could be found or if the temperature level of the high pressure cycle could be increased **during** production. Moreover, in future low-exergy consumers and storage systems will be available for heating systems and buildings so that more energy can be saved. Currently, 47.68 €/h have to be invested in the refrigeration system (and 16.77 €/h in the DHW system, resp.).

# 6 Improvement Measures and Component Optimisation

From the exergy-analysis follows that a higher condensation pressure offers a higher potential for heat reclaim. This is only worthwhile if the DHW consumption is high enough. Therefore a mass flow depending control for the cooling towers is implemented. During production the saturation temperature is lifted by a throttling of the tower ventilation from a max. value of 10 bar to 14 bar. Outside production times it is important to achieve low condensation pressures (min. 7 bar) in order to reduce the power consumption (see Fig.8).

Additionally, the compressor cascade is changed so that the base requirement in winter is provided by the smallest compressor because the COP is generally better with a higher part load factor. In summer the cascade order remains the same because the base load for cooling storage rooms is often higher than the maximum capacity of the smallest compressor.

For both periods in summer and winter the running costs can be reduced by 4 % (see Tab. 5) due to the increased heat recovery (≈ 20 %) at a slightly higher power consumption (1 to 2 %). For those savings there are basically no large investments needed. Compared to the running costs of the refrigeration plant (≈ 200.000 €/a) for one year the possible reduction is 5.000 €/a.

The simulation of one week takes 12 hours on a fast PC (3 GHz processor) due to on/off-control of the

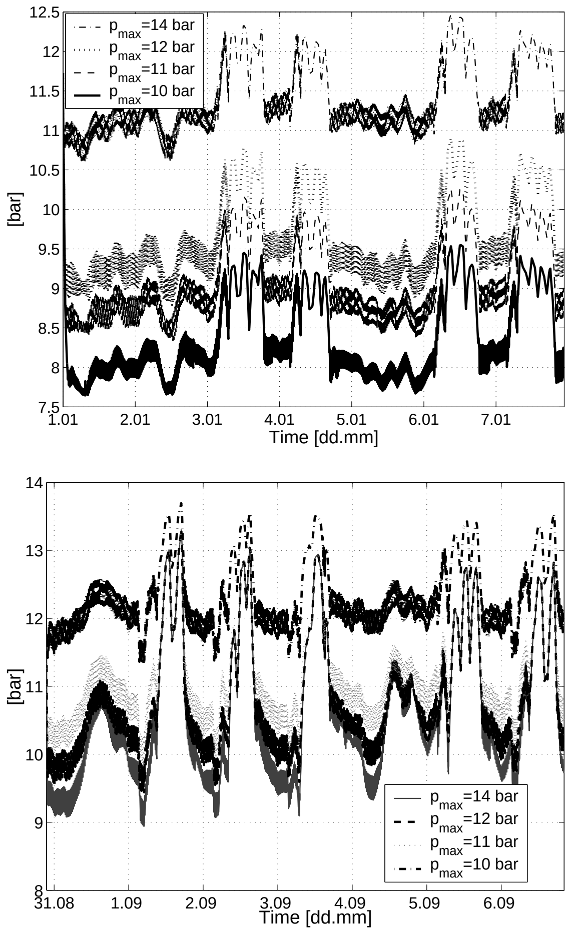


Figure 8: Impact of the variable cooling tower control on the condensation pressure in January (t.) and September (b.)

compressors at part load. If frequent events could be avoided by a part load function or if a higher plant utilisation is considered the simulation time would be reduced to approximately 1 hour.

## 7 Conclusions and Outlook

It is possible to simulate even complex refrigeration plants for longer periods like weeks with a high amount of unsteady events resulting from a 2-point-control of some components. A modelling approach aiming to further reduce events during simulation (e. g., performance curves for on/off-controlled elements) would yield faster simulation times for calculating balances of whole years. Attaining this goal is important since the boundary conditions profile (test reference year) has a dominating influence on the total power consumption.

| Mode | Jan. act. | Jan. mod. | Sep. act. | Sep. mod. |
|---|---|---|---|---|
| **Power con.** [kWh] | 46.285 | 46.887 | 60.123 | 61.319 |
| **Fresh water** [$m^3$] | 118 | 126 | 346 | 310 |
| **Waste water** [$m^3$] | 39 | 42 | 115 | 103 |
| **Heat reclaim** [kWh] | 22.795 | 27.127 | 29.966 | 34.241 |
| **Costs** [€] | 2.557 | 2.446 | 3.627 | 3.487 |
| **Rel. dev.** [%] | - | -4.3 | - | -3.9 |

Table 5: Comparison of power and water consumption, heat reclaim and running costs for one week in January and September of the actual and modified plant

When considering multiple consumers (e. g., refrigeration at different temperature levels, DHW) the system's control is a key factor for realising an efficient plant operation. In this paper, it was shown that in even well-designed plants incorporating state-of-the-art subcomponents savings are attainable without much capital investment. The transient simulation offers a method for a holistic analysis of technical systems throughout the product-life-cycle. In combination with an exergy-analysis it is possible to find optimisation potential for characteristic operating points. Basically, the implementation of the exergy method is easy when necessary medium properties are provided by the control volume models (see Eq. 16). Nevertheless, the evaluation may become tedious for complex dynamic systems especially when economical constraints (energy or exergy costs) have to be considered. For this purpose capable validation and evaluation methods must be implemented to concisely provide the information needed for drawing correct conclusions and finding effective improvement measures.

## References


[1] A. Bejan, G. Tsatsaronis, and M. Moran. *Thermal Design and Optimization*. John Wiley & Sons, New York/Chichester/Brisbane, 1996.

[2] V. M. Brodyansky, M. V. Sorin, and P. Le Goff. *The efficiency of industrial processes: Exergy analysis and optimization*. Elsevier, Amsterdam / London / New York, 1994.

[3] St. Wischhusen and G. Schmitz. Transient simulation as an economical analysis method for energy supply

systems for building or industry. *Applied Thermal Engineering*, 24:2157 – 2170, 2004.

[4] St. Wischhusen and G. Schmitz. Numerical Simulation of Complex Cooling and Heating Systems. In *Proceedings of the 2nd Int. Modelica-Conference*, pages pp. 183–191, Oberpfaffenhofen, 2002. Modelica Association.

[5] St. Wischhusen, B. Lüdemann, and G. Schmitz. Halbhermetische hubkolbenverdichter. In *Proceedings of the 3rd Modelica Conference*, pages pp. 259–267, Linköping, Schweden, 2003. Modelica Association.

[6] T. Pfafferott. *Dynamische Simulation von $CO_2$-Kälteprozessen für mobile Anwendungen*. Shaker Verlag, Aachen, 2005.

[7] H.-D. Baehr and R. Tillner-Roth. *Thermodynamische Eigenschaften umweltverträglicher Kältemittel*. Springer Verlag, Berlin, 1995.

[8] J. M. Jensen. *Dynamic modeling of Thermo-Fluid Systems - With focus on evaporators for refrigeration*. Department of Mechanical Engineering, Technical University of Denmark, Lyngby (Dänemark), 2003.

[9] R. Shah and D. Sekulić. *Fundamentals of Heat Exchanger Design*. John Wiley & Sons, Hoboken, USA, 2003.

[10] W. Stoecker. *Industrial Refrigeration Handbook*. McGraw–Hill, New York/San Francisco/Washington D. C., USA, 1998.

[11] W. Leidenfrost and B. Korenic. Experimentelle Überprüfung einer Berechnungsmethode für die Leistungsvoraussage verdunstungsgekühlter Kondensatoren. *Brennstoff–Wärme–Kraft*, 34(1):9–14, 1982.

[12] H.-M. Hellmann. *Untersuchung und einheitliche Berechnung des Betriebsverhaltens von Verdunstungskühlern und –kondensatoren*. Phd thesis, Technische Universität Braunschweig, Braunschweig, 1991.

[13] P. Stabat and D. Marchio. Simplified model for indirect-contact evaporative cooling-tower behaviour. *Applied Energy*, 78:433–451, 2004.

[14] T. Helmke. $NH_3$-Verbundkälteanlagen mit Schraubenverdichtern kleiner Leistung. *KK - Die Kälte- und Klimatechnik*, (5), 2000.